Materials Characterization 140 (2018) 197–206

Contents lists available at ScienceDirect

Materials Characterization

journal homepage: www.elsevier.com/locate/matchar

Influencing mechanism of Al-containing Zn coating on interfacial microstructure and mechanical properties of friction stir spot welded Mg–steel joint

R.Z. Xu[a,b], D.R. Ni[a], Q. Yang[a], B.L. Xiao[a], C.Z. Liu[b], Z.Y. Ma[a,*]

[a] Shenyang National Laboratory for Materials Science, Institute of Metal Research, Chinese Academy of Sciences, 72 Wenhua Road, Shenyang 110016, China
[b] College of Material Science and Engineering, Shenyang Aerospace University, 37 Daoyi South Street, Shenyang 110136, China

ARTICLE INFO

Keywords:
Friction stir spot welding
Dissimilar metals
Zn-Al coating
Intermetallic compound
Metallurgical bonding

ABSTRACT

2.4 mm thick AZ31 Mg alloy sheet and 1.5 mm Q234 steel sheet with a hot-dipped Al-containing Zn coating were friction stir spot welded (FSSW) using a pinless tool. It was shown that the Al-containing Zn coating played a crucial role in joining the Mg alloy and steel during FSSW. The Zn coating observably improved the Mg–steel interfacial wettability during FSSW, and the Al_5Fe_2 phase in the Zn coating on the steel substrate surface promoted the metallurgical bonding of Mg alloy and steel. It was confirmed that the Al_5Fe_2 phase on the steel surface resulted from the reaction between the steel substrate and the Al in the Zn coating during hot-dipping, and was not related to the Al-containing Mg alloy substrate. The tensile-shear load of the FSSW Mg–steel joint reached 4.3 kN. The fracture of the joint occurred along the interface on the steel substrate side. The interface between the Al_5Fe_2 layer and Mg alloy substrate was the weakest region of the Mg–steel joint.

1. Introduction

In order to reduce vehicle weight and to save energy, special attention has been paid to hybrid structural components that take advantage of dissimilar metals [1,2]. In particular, composite structures consisting of ultra-lightweight Mg alloys and steels are considered promising for automotive applications. Among various manufacturing techniques, welding is one of the widely used methods for preparing the Mg–steel composite structures [3–8].

However, the marked differences in the metallurgical and physical properties between Mg alloys and steels, such as considerable melting point difference, almost no intersolubility, and no Mg—Fe intermetallic compound (IMC), resulted in the significantly increased difficulty of Mg–steel welding [9,10]. Previous studies have shown that Mg alloys and steels could be successfully joined using resistance spot welding [11,12], ultrasonic spot welding [13–15], laser welding [16,17], and laser-tungsten inert gas hybrid welding [18]. It was believed that the bond between Mg alloys and steels was achieved through Al—Fe IMCs [11,12,16–18]. Therefore, Al was considered as a necessary alloying element in Mg alloys for successful Mg–steel welds.

In the above-mentioned welding processes, it was reported that Al diffused from the Mg substrate to the Fe surface, thereby creating a metallurgical bonding between Mg alloys and steels by means of reaction between Al and Fe. Therefore, controlling the precipitation of Al from the Mg alloy substrate is a key factor for Mg–steel welding, which undoubtedly increases the difficulty of achieving optimal welds [19,20]. Furthermore, it is considered that the presence of a Zn coating is essential for the elimination of the negative effects of oxides during the welding process [11,18–21].

Friction stir spot welding (FSSW) is a new welding method, developed based on the friction stir welding technique [22,23]. As a solid state joining method, FSSW integrates the advantages of minimal thermal deformation, sound mechanical properties and green welding processes, and therefore has received considerable attention in the welding of dissimilar metals such as Mg alloy and steel [24].

The short heating time and the low heat input make FSSW more energy efficient and cleaner than other spot welding techniques [25,26]. However, the low welding temperature is liable to increase the difficulty of Al diffusion from the Mg alloy substrate to the steel sheet surface [27–29], thereby influencing the Mg–steel metallurgical bonding during FSSW. For example, in the AM60 (upper sheet)–DP600 dual phase steel FSSW joint, there was no evidence of IMC formation, so only a mechanical bond formed between the Mg alloy and steel. In addition, pure Zn coating on the DP600 steel surface did not promote Mg–steel interfacial bonding, but actually increased the cracking at the interface due to the influence of Zn in facilitating local melting [30].

* Corresponding author.
E-mail address: zyma@imr.ac.cn (Z.Y. Ma).

https://doi.org/10.1016/j.matchar.2018.04.011
Received 4 January 2018; Received in revised form 5 April 2018; Accepted 6 April 2018
Available online 09 April 2018

Table 1
Welding parameters for FSSW of Mg–steel.

Plunge depth (mm)	Plunge rate (mm/s)	Rotation rate (rpm)	Dwell time (s)	Withdrawing rate (mm/s)
1.0	2.5	3000	5.0	3.0

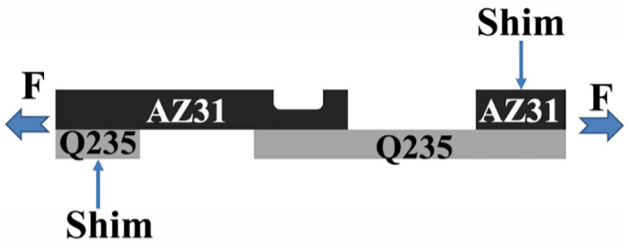

Fig. 1. Schematic of the tensile shear test specimens.

In FSSW, the pressure, reaction temperature and time required by the diffusion reaction among the Mg alloy, coating and steel are provided by the action of the rotation, plunge and dwelling of the stirring tool [31]. Therefore, knowing how to provide the Al element for the interfacial reaction is the key to realizing metallurgical bonding between Mg alloy and steel in FSSW. In fact, in a hot-dip galvanized process, a small quantity of Al is usually added to the Zn coating, forming Al-containing Zn coating [32]. Therefore, Al in the Zn coating may be beneficial to joining of the Mg and steel, thereby improving the mechanical properties of the FSSW joints.

In order to verify the beneficial effect of Al in the Zn coating on the Mg–steel joint, a steel sheet with a hot-dipped Al-containing Zn coating was selected for joining Mg alloy and steel by FSSW, with the goal of realizing the metallurgical bonding of Mg–steel. Pinless FSSW [21] was applied to increase the bonding area of the Mg–steel joint and reduce

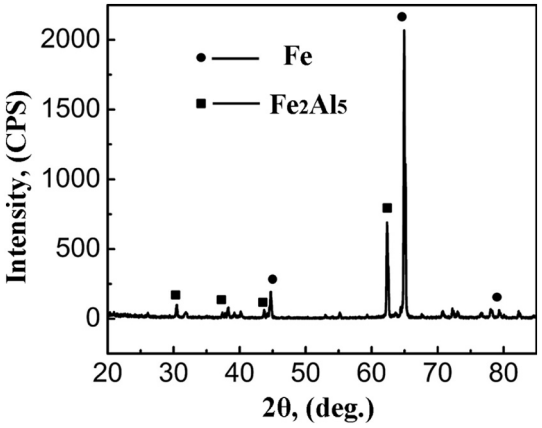

Fig. 4. X-ray result of Zn—Al coated steel surface after etching by fuming HNO_3.

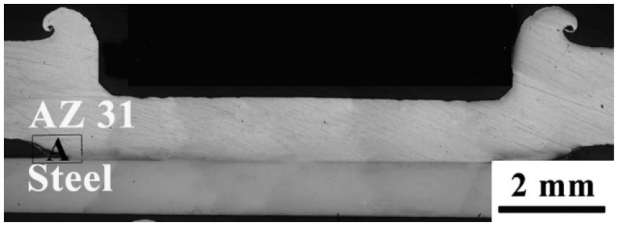

Fig. 5. Typical cross-section photograph of FSSW Mg–steel joint.

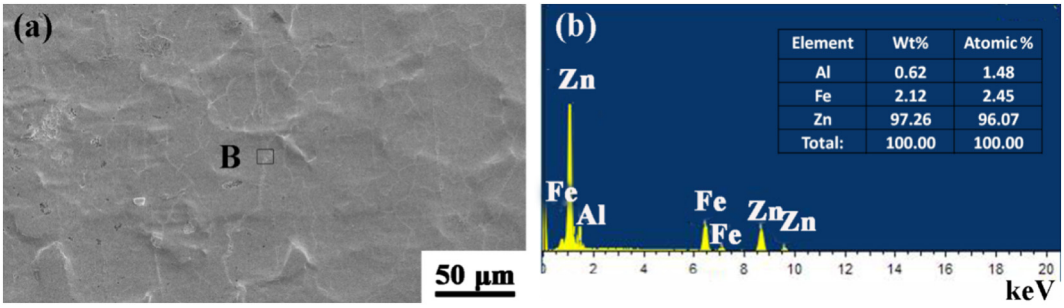

Fig. 2. (a) SEM micrograph of coating surface on Q235 steel and (b) EDS spectra obtained from zone B in panel a.

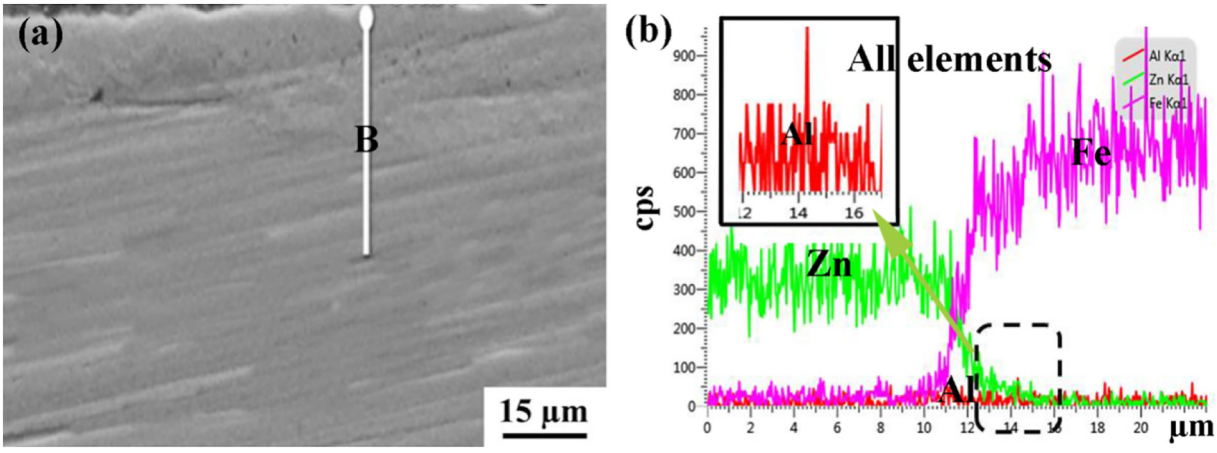

Fig. 3. (a) SEM micrograph of cross-sectioned Zn—Al coated steel and (b) elemental analysis of line B in panel a.

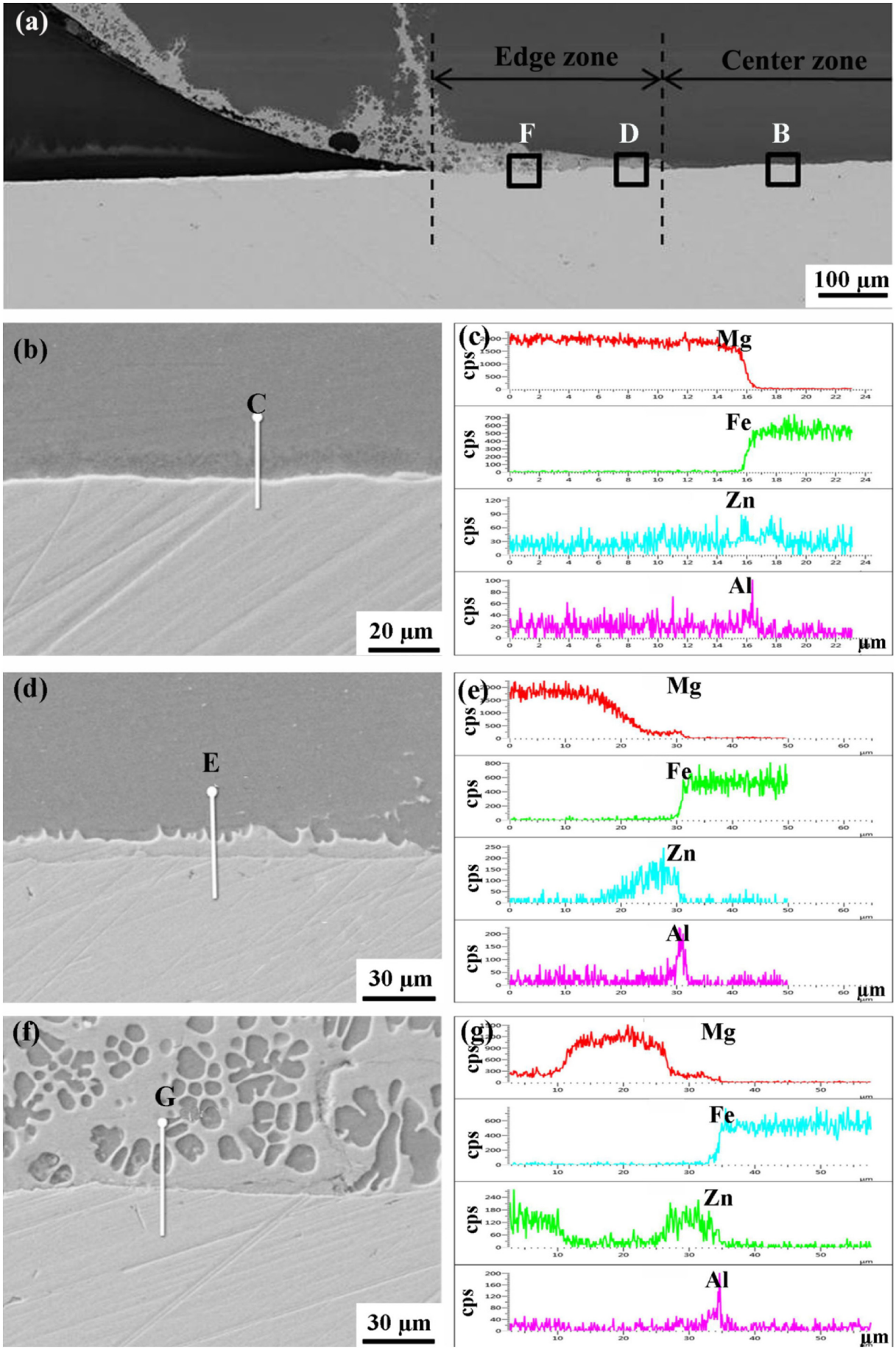

(caption on next page)

Fig. 6. (a) Microstructure of region A in Fig. 5 and (b)–(g) microstructures and elemental line analyses of different zones in Fig. 6a: (b) region B and (c) line C; (d) region D and (e) line E; (f) region F and (g) line G.

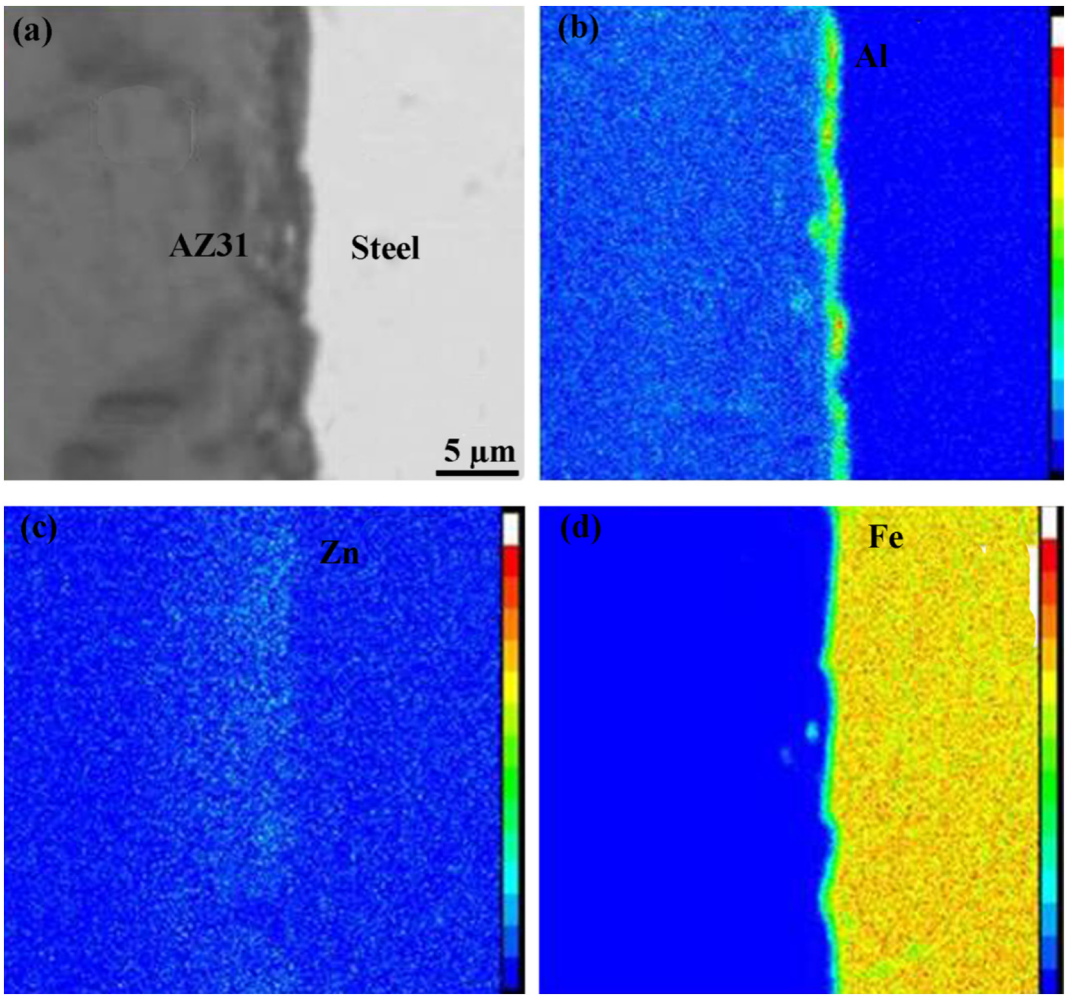

Fig. 7. (a) Mg–steel interface in the center zone of a FSSW joint, and elemental distribution of (b) Al, (c), Zn, (d) Fe.

the abrasion of the stirring tool. The influencing mechanism of the Al-containing Zn coating on the interfacial reaction and the mechanical properties of the FSSW joint were investigated in detail.

2. Experimental

The base materials were 2.4 mm thick hot-rolled AZ31 Mg sheet, with chemical compositions of Mg–2.74Al–0.31Zn–0.13Mn–0.01Si (at. %), and 1.5 mm thick hot-dipped Zn−Al Q235 steel sheet, with compositions of Fe–0.92C–0.40Mn–0.32Si (at.%). During FSSW, AZ31 sheet was lapped on top of the Q235 steel by a holding fixture. The FSSW operation was conducted using a pinless welding tool with a 10 mm diameter shoulder. The specific welding parameters are depicted in Table 1.

Microstructural examinations were conducted using optical microscopy (OM), scanning electron microscopy (SEM, LEO Supra 35) with energy-dispersive X-ray spectroscopy (EDS), electron probe micro-analysis (EPMA, Shimadzu 1610) and transmission electron microscopy (TEM, Tecnai F20). The specimens were sectioned parallel to the loading direction through the center of the joints. After being mechanically ground and polished, the specimens were etched using an etching reagent consisting of 4.2 g picric acid, 10 ml acetic acid, 10 ml H_2O, and 70 ml ethanol. Furthermore, the coated steel sheet was etched by fuming HNO_3 and then analyzed by X-ray diffraction (XRD) using CuKα radiation.

Lap-shear tensile specimens were formed by electrical discharge machining of the FSSW joint, with a length of 100 mm, a width of 30 mm and an overlap area of 30 × 30 mm. Shims were used at each end of the specimens to ensure tensile shear loads in the FSSW joint as shown in Fig. 1. Lap-shear tensile tests were conducted using a Zwick/Roell Z050 tester at a tensile speed of 0.5 mm/min. The load values were obtained by averaging three test results. The fracture location and characteristics were examined by OM and SEM.

3. Results and Discussion

3.1. Characteristics of Hot-dipped Al-containing Zn Coating

Fig. 2a and b shows SEM micrographs, of the coating surface on the Q235 steel, and of the EDS spectra obtained from zone B in Fig. 2a,

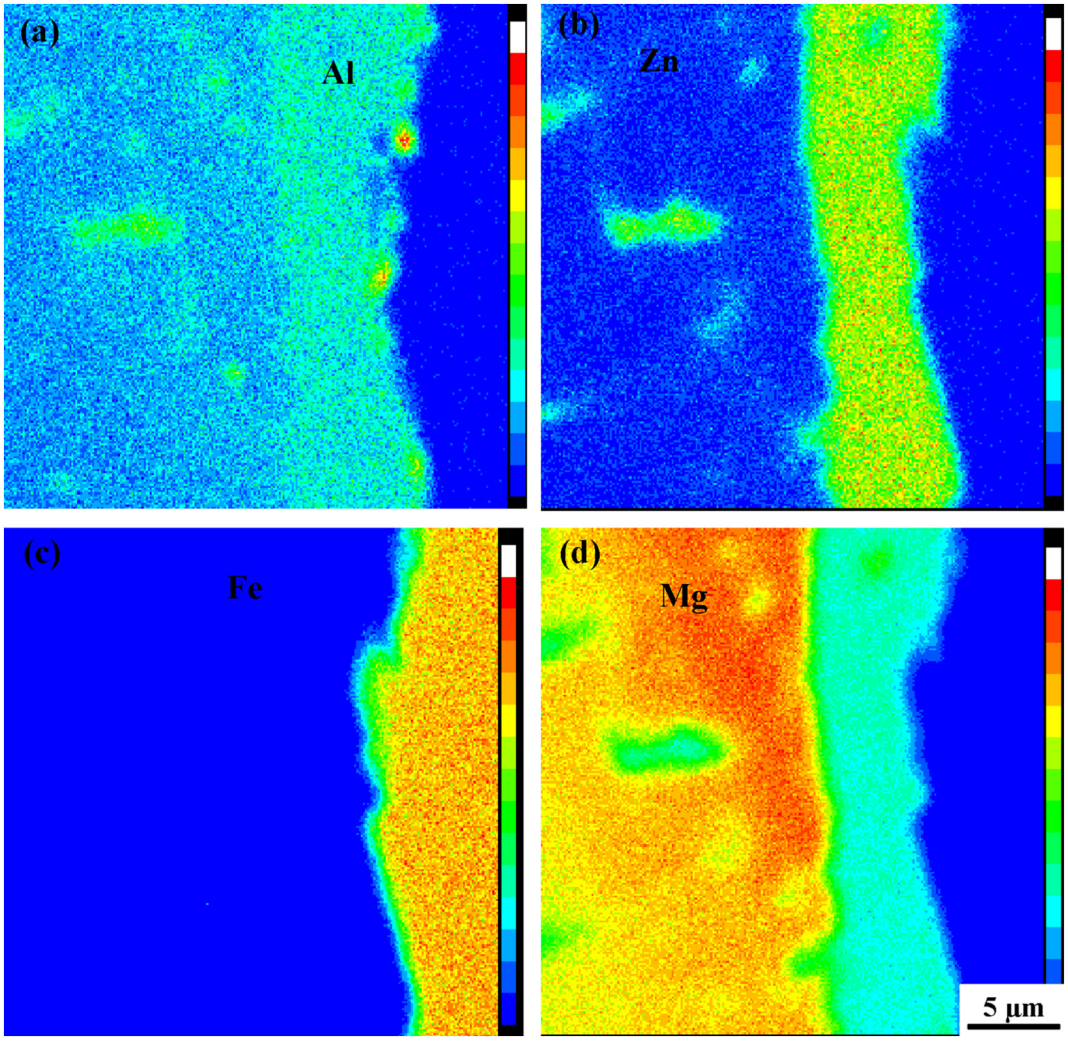

Fig. 8. Elemental distribution of Mg–steel interface in the edge zone of a FSSW joint: (a) Al, (b) Zn, (c) Fe, and (d) Mg.

respectively. The chemical composition of point B was determined to be 96.07 at.% Zn, 2.45 at.% Fe and 1.48 at.% Al. This proves that the coating contained a small quantity of Al.

Fig. 3a shows a SEM micrograph of cross-sectioned Zn—Al coated steel. It can be seen that the thickness of the coating was approximately 15 μm. Line scan analysis of the coating shown in Fig. 3a indicated that Al was rich at the interface between the Zn coating and steel (Fig. 3b). The XRD analyses on the surface of the coating after etching by fuming HNO_3 indicated the existence of Al_5Fe_2 on the surface of the steel sheet (Fig. 4). This indicates that the interface between the coating and steel was composed of ultra-thin Al_5Fe_2 IMCs rather than Zn—Fe IMCs. The Al_5Fe_2 IMCs were believed to form during the hot-dip galvanizing process.

3.2. FSSW of Mg–steel Dissimilar Metals

3.2.1. Macrostructure and Microstructure of the Mg–steel Joint

Fig. 5 shows a typical cross-sectional photograph of the FSSW Mg–steel joint. It is clear that AZ31 Mg alloy sheet and Q235 steel sheet were joined together by FSSW. Fig. 6a shows the SEM micrograph of the FSSW Mg–steel joint in zone A of Fig. 5a. It is noted that the joint region could be generally divided into the center zone and the edge zone. A continuous reaction layer appeared at the Mg–steel interface. In addition, the thickness of the reaction layer decreased from the edge zone to the center zone of the joint as shown in Fig. 6b, d and f.

Representative line analyses of Mg, Fe, Zn and Al across the interface between AZ31 and steel are shown in Fig. 6c, e and g. It was found that Al was rich at the interface between Mg alloy and steel, but no significant Zn was found on the steel side of the interface. In addition, the microstructure and EDS line analysis results shown in Fig. 6f and g revealed that Mg—Zn IMCs formed on the Mg alloy side in the edge zone. Elemental mapping for the interfaces of the center zone and edge zone confirmed that the Al-rich layer was uniform and continuous as shown in Figs. 7 and 8.

The microstructure and phase composition at the interface were further examined by TEM. Fig. 9a shows the TEM microstructure of the interface in the center zone. An ultra-thin reaction layer, about 100 nm in thickness, was clearly observed at the interface. EDS analysis results indicated that region B with compositions of 96.4 at.% Mg, 2.5 at.% Al and 1.1 at.% Zn (Fig. 9b) should be AZ31 and region E with

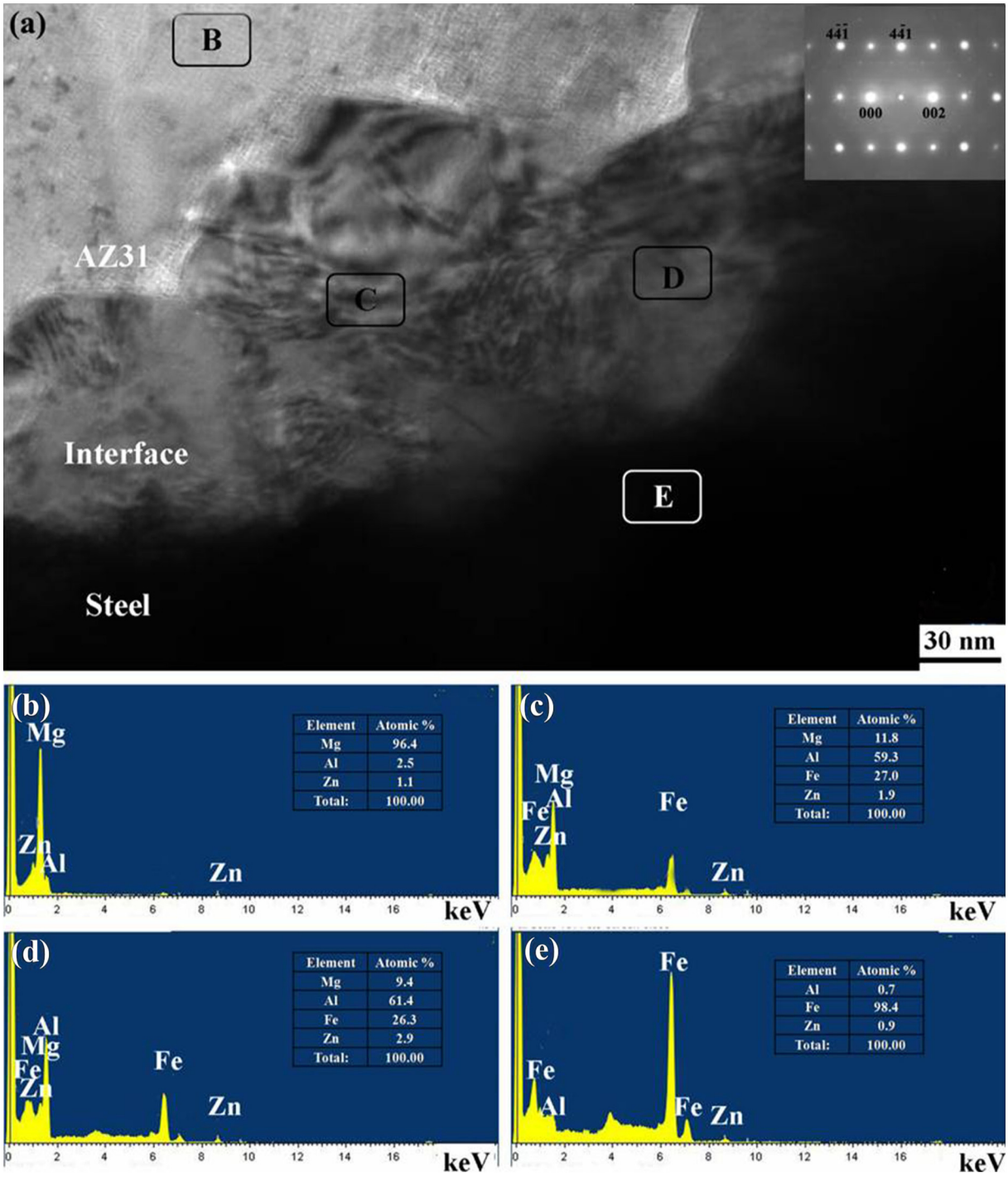

Fig. 9. (a) TEM microstructure of interface in the center zone and EDS spectra obtained from regions (b) B, (c) C, (d) D, and (e) E in panel a.

compositions of 98.4 at.% Fe, 0.7 at.% Al and 0.9 at.% Zn (Fig. 9e) should be steel.

Between regions B (Mg) and E (steel), two regions in the reaction layer were analyzed; region C, with compositions of 11.8 at.% Mg, 59.3 at.% Al, 27.0 at.% Fe and 1.9 at.% Zn (Fig. 9c), and region D, with compositions of 9.4 at.% Mg, 61.4 at.% Al, 26.3 at.% Fe and 2.9 at.% Zn (Fig. 9d). These areas should correspond to an IMC, however, the IMC area was too small for their composition to be accurately reflected by EDS. The selected area electron diffraction (inset in Fig. 9a) revealed that the IMC at the interface between the Mg alloy and steel in the center zone was Al_5Fe_2.

The TEM microstructure of the interface (Fig. 10a), the EDS result (Fig. 10b) and the selected area electron diffraction (inset in Fig. 10a) in the edge zone all proved that the IMC layer next to the steel side was

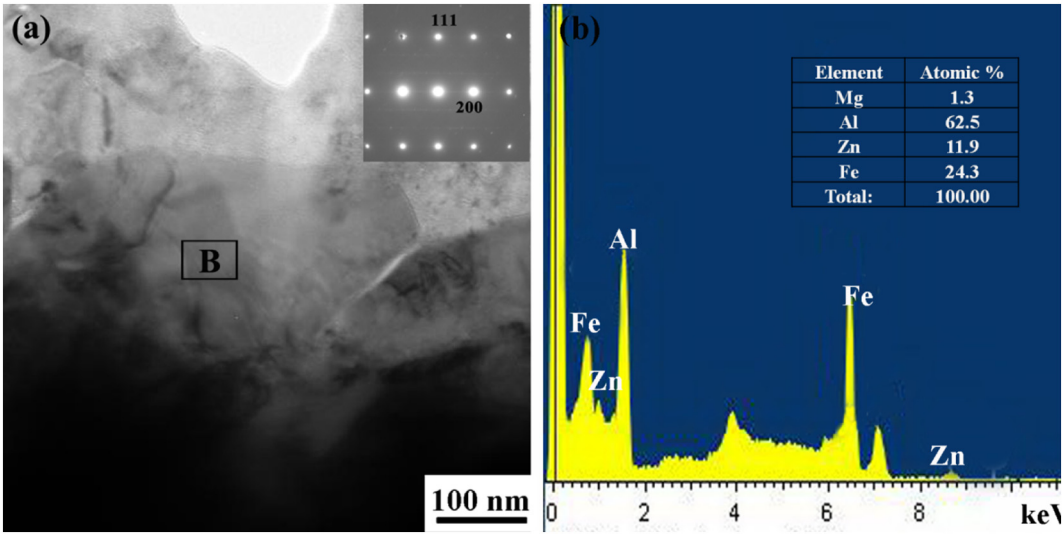

Fig. 10. (a) TEM microstructure of interface in the edge zone and (b) EDS spectra obtained from region B in panel a.

Al_5Fe_2, similar to that in the center zone.

In brief, a metallurgical bond was formed between the AZ31 Mg alloy and Zn−Al coated Q235 steel during FSSW, and the IMC phase of the interfacial zone was Al_5Fe_2.

3.2.2. Properties and Fracture Characteristics of Mg–steel Joint

The tensile-shear test revealed that the load on the joint could reach 4.3 kN. Fig. 11a shows the typical fracture location of the FSSW Mg–steel joint. It was found that fracture of the joint occurred along the interface between Mg alloy and steel (Fig. 11c and e). Fig. 11b shows the SEM macrograph of the fracture surface of the Mg–steel joint on the steel side, divided into two different zones from the center to the edge of joint according to the different surface macrographs, which agrees with the result of Fig. 6a.

Fig. 11d and f show magnified images of regions D and F as denoted in Fig. 10b, respectively. The quite-smooth fracture surface on the steel side suggests the brittle fracture characteristics of the joint. EDS analysis revealed that region A in Fig. 11f consisted of 6.7 at.% Mg, 36.9 at.% Al, 55.9 at.% Fe and 0.5 at.% Zn (Fig. 12a) and region B in Fig. 11d was composed of 3.8 at.% Mg, 28.2 at.% Al, 67.4 at.% Fe and 0.6 at.% Zn (Fig. 12b). Because EDS X-rays could penetrate the extremely thin IMC layer, the percentage of Al determined by EDS was lower than that in the Al−Fe IMC.

Based on the fractography and EDS analyses, it was further confirmed that the transitional layer between Mg and steel was Al−Fe IMC. In addition, it was concluded that the fracture of the joint initiated along the interface between the reaction layer and the steel that was the weakest region of the joint.

3.3. Influencing Mechanism of Al-containing Zn Coating on FSSW AZ31-Q235 Joint

In the hot-dipped Al-containing Zn coating on the steel surface, Al_5Fe_2 formed at the interface between the coating and steel before FSSW (Figs. 2, 3 and 4). As a solid state joining method, the welding temperature of FSSW is lower than the melting point of AZ31 Mg alloy, so the Al_5Fe_2 phase adjacent to the steel substrate remained after FSSW due to its relatively high melting point (1169 °C) as shown in Figs. 9 and 10. However, Zn was melted and then squeezed out of the center zone due to the action of the rotation, plunge and dwelling of the stirring tool. Thus, Zn was only rich in the edge zone as shown in Figs. 6e, g and 8b, and there was no Zn at the interface next to the steel side. More importantly, the melted Zn was difficult to diffuse into the AZ31 due to relatively low process temperature and short duration. Considering that the joint was predominantly composed of the center zone, the effect of liquid metal embrittlement from Zn on the fracture of the joint was negligible.

Based on the analyses above, the joining mechanism of Mg to Zn−Al coated steel by FSSW can be elucidated schematically in Fig. 13. First, the Al-containing Zn coating on the steel surface was melted under the thermo-mechanical action of the stirring tool as shown in Fig. 13a and b. Second, the melted Al-containing Zn coating was squeezed out of the bonded region, allowing fresh Mg surface to directly contact Al_5Fe_2 IMC layer, thus creating a condition similar to vacuum diffusion welding [11,17,19]. In this case, no metallic oxides formed at the faying interface during FSSW (Figs. 6, 9, 10 and 12). Therefore, Zn coating improved the wettability of the joining interface between Mg alloy and steel. Third, the liquid Zn flowed from the center zone to the edge zone of the FSSW joint, leading to a Zn-rich region (edge zone) as shown in Fig. 13c and d. Finally, the pre-existing Al_5Fe_2 phase remained in the interface zone and bonded with AZ31 Mg alloy and steel. This was why the weakest zone was at the AZ31–Al_5Fe_2 interface (Fig. 13d).

In short, the Al-containing Zn coating played a dual role in joining the Mg alloy and steel during FSSW. On the one hand, the coating that was squeezed out of the bonded region did not contribute to the interfacial reaction product, but it observably improved interfacial wettability. On the other hand, the pre-existing Al_5Fe_2 phase contributed to the metallurgical bonding of Mg alloy and steel.

4. Conclusions

In this study, the effect of the hot-dipped Al-containing Zn coating on the microstructural features and mechanical properties of the FSSW AZ31–steel joint was investigated; the following conclusions were drawn:

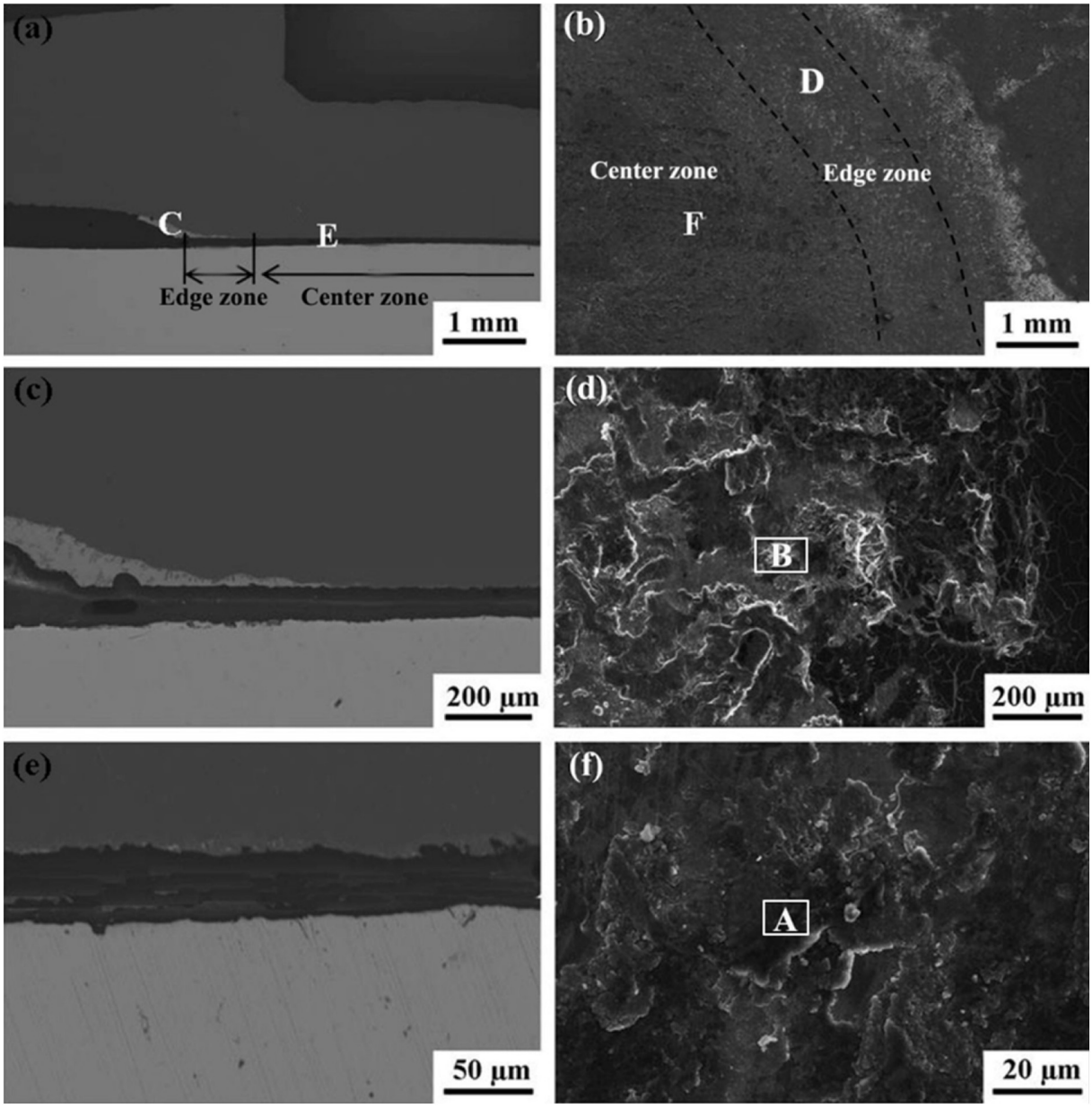

Fig. 11. (a) Typical fracture location of FSSW Mg–steel joint and magnified graphs of region (c) C and region (e) E in panel a; (b) SEM image of facture surface and magnified graphs of region (d) D and region (f) F in panel b.

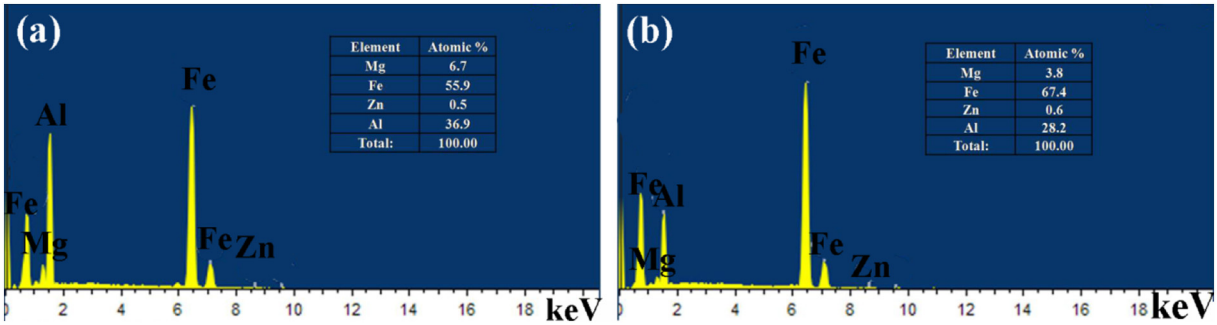

Fig. 12. EDS spectra obtained from (a) region A in Fig. 11f and (b) region B in Fig. 11d.

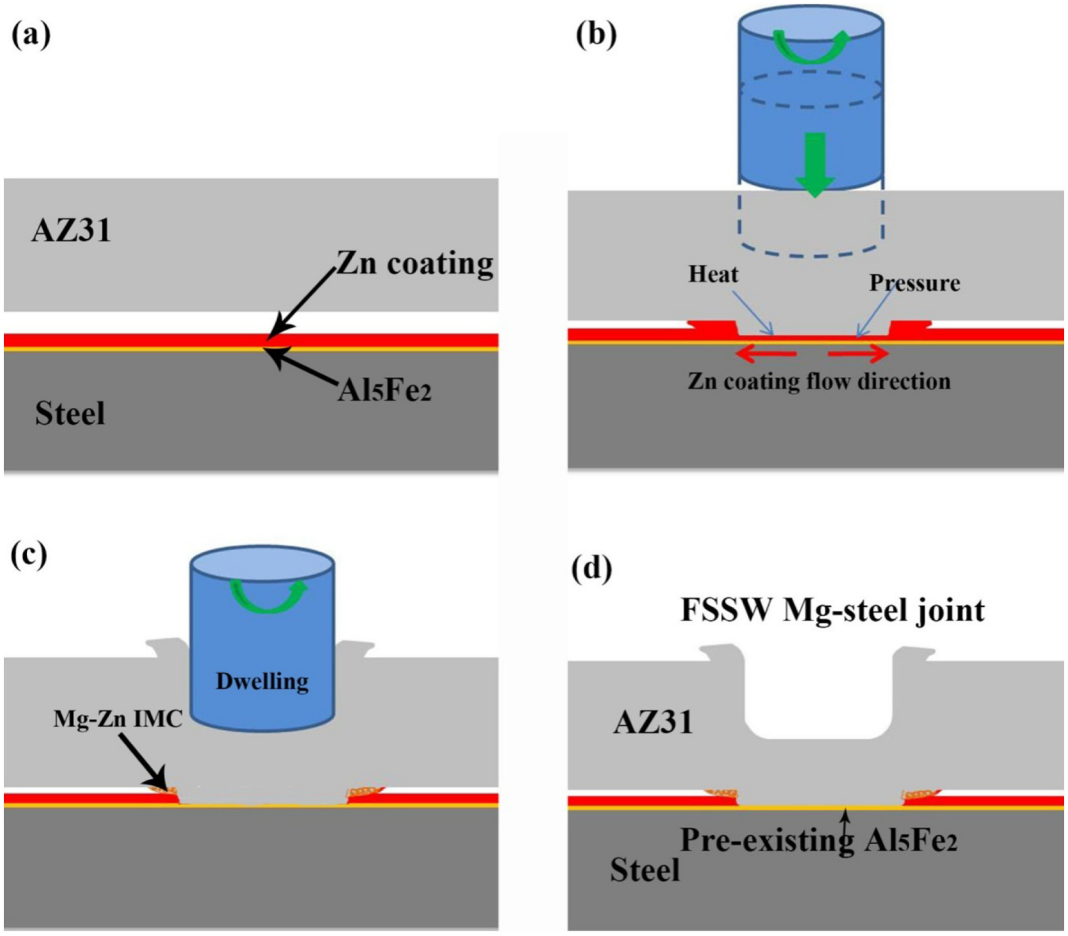

Fig. 13. Schematic of joining process between Mg and Zn−Al coated steel by FSSW: (a) Zn−Al coating characteristic, (b) squeezing out and (c) reaction of Zn coating with substrates, and (d) formed joint.

(1) In the hot-dipped Al-containing Zn coating of steel sheet, Al from the Zn coating was rich at the interface between the coating and steel, thus forming Al_5Fe_2 phase on the surface of the steel sheet.
(2) During FSSW, the coating that was squeezed out of the bonded region did not contribute to the interfacial reaction, but it observably improved the interfacial wettability.
(3) The pre-existing Al_5Fe_2 phase on the surface of the steel sheet remained at the interface between the Mg alloy and steel during FSSW, and contributed to achieving metallurgical bonding between the Mg alloy and steel.
(4) The tensile-shear load of the FSSW AZ31–steel joint reached 4.3 kN. The fracture of the joint occurred along the interface next to the steel side, with the interface between the Al_5Fe_2 IMC layer and the Mg alloy substrate being the weakest region of the joint.

Acknowledgments

This study was supported by the National Natural Science Foundation of China under Grant Nos. 51601121 and 51331008, and Natural Science Foundation of Liaoning Province Program Nos. L201624 and 201602570.

References

[1] P. Xue, B.L. Xiao, Z.Y. Ma, Effect of interface microstructure evolution on mechanical properties and fracture behavior of friction stir welded Al-Cu joints, Metall. Mater. Trans. A 46 (2015) 3091–3103.
[2] R. Qiu, C. Iwamoto, S. Satonaka, Interfacial microstructure and strength of steel-aluminum alloy joints welded by resistance spot welding with cover plate, J. Mater. Process. Technol. 209 (2009) 4186–4193.
[3] P.B. Prangnell, F. Haddadi, Y.C. Chen, Ultrasonic spot welding aluminum to steel for automotive applications-microstructure and optimization, Mater. Sci. Technol. 27 (2011) 617–624.
[4] M. Elthalabawy, I.K. Tahir, Eutectic bonding of austenitic stainless steel 316L to magnesium alloy AZ31 using copper interlayer, Int. J. Adv. Manuf. Technol. 55 (2011) 235–241.
[5] M. Ding, Y. Zhen, J. Lian, Dissimilar spot welding joints of AZ31-443 ferritic stainless steel with cover plate, Int. J. Adv. Manuf. Technol. 85 (2016) 1539–1545.
[6] R. Cao, Q.W. Xu, H.X. Zhu, G.J. Mao, Q. Lin, P. Wang, Weldability and distortion of Mg AZ31-to-galvanized steel plug welding joint by cold metal transfer method, J. Manuf. Sci. E. T. ASME 139 (2017) 02100101–02100110.
[7] H. Wang, G. Song, Influence of adhesive and Ni on the interface between Mg and Fe in the laser-TIG-adhesive hybrid welding joint, Int. J. Precis. Eng. Manuf. 17 (2016) 823–827.
[8] G. Song, T. Li, Z. Zhang, L. Liu, Investigation of unequal thickness Mg/steel butt-welded plate by hybrid laser-tungsten inert gas welding with a Ni interlayer, J. Manuf. Process. 30 (2017) 299–302.
[9] D. Ren, L. Liu, Interface microstructure and mechanical properties of arc spot welding Mg–steel dissimilar joint with Cu interlayer, Mater. Des. 59 (2014) 369–376.
[10] G. Song, G. An, L. Liu, Effect of gradient thermal distribution on butt joining of magnesium alloy to steel with Cu-Zn alloy interlayer by hybrid laser-tungsten inert gas welding, Mater. Des. 35 (2012) 323–329.
[11] L. Liu, L. Xiao, J.C. Feng, Y.H. Tian, S.Q. Zhou, Y. Zhou, The mechanisms of resistance spot welding of magnesium to steel, Metall. Mater. Trans. A 41 (2010) 2651–2661.
[12] L. Liu, L. Xiao, D.L. Chen, J.C. Feng, S. Kim, Y. Zhou, Microstructure and fatigue properties of Mg-to-steel dissimilar resistance spot welds, Mater. Des. 45 (2013) 336–342.
[13] V.K. Patel, S.D. Bhole, D.L. Chen, Formation of zinc interlayer texture during dissimilar ultrasonic spot welding of magnesium and high strength low alloy steel, Mater. Des. 45 (2013) 236–240.
[14] V.K. Patel, S.D. Bhole, D.L. Chen, Characterization of ultrasonic spot welded joints of Mg-to-galvanized and ungalvanized steel with a tin interlayer, J. Mater. Process. Technol. 214 (2014) 811–817.
[15] V.K. Patel, D.L. Chen, S.D. Bhole, Dissimilar ultrasonic spot welding of Mg-Al and Mg-high strength low alloy steel, Theor. Appl. Mech. Lett. 4 (2014) 0410051–0410058.
[16] Y. Miao, D. Han, J. Yao, F. Li, Effect of laser offsets on joint performance of laser penetration brazing for magnesium alloy and steel, Mater. Des. 31 (2010) 3121–3126.
[17] M. Wahba, S. Katayam, Laser welding of AZ31B magnesium alloy to Zn-coated steel, Mater. Des. 35 (2012) 701–706.
[18] C. Tan, L. Li, Y. Chen, W. Guo, Laser-tungsten inert gas hybrid welding of dissimilar metals AZ31B Mg alloys to Zn coated steel, Mater. Des. 49 (2013) 766–773.

[19] L. Li, C. Tan, Y. Chen, CO_2 laser welding-brazing characteristics of dissimilar metals AZ31B Mg alloy to Zn coated dual phase steel with Mg based filler, J. Mater. Sci. Technol. 213 (2013) 361–375.
[20] C. Tan, L. Li, Y. Chen, C. Mei, W. Guo, Interfacial microstructure and fracture behavior of laser welded-brazed Mg alloys to Zn-coated steel, Int. J. Adv. Manuf. Technol. 68 (2013) 1179–1188.
[21] R.Z. Xu, D.R. Ni, Q. Yang, C.Z. Liu, Z.Y. Ma, Pinless friction stir spot welding of Mg-3Al-1Zn alloy with Zn interlayer, J. Mater. Sci. Technol. 32 (2016) 76–88.
[22] S. Lathabai, M.J. Painter, G.M.D. Cantin, V.K. Tyagi, Friction spot joining of an extruded Al-Mg-Si alloy, Scr. Mater. 55 (2006) 899–902.
[23] A. Gerlich, P. Su, T.H. North, Tool penetration during friction stir spot welding of Al and Mg alloys, J. Mater. Sci. 40 (2005) 6473–6479.
[24] Y. Uematsu, T. Kakiuchi, Y. Tozaki, H. Kojin, Comparative study of fatigue behaviour in dissimilar Al alloy/steel and Mg alloy/steel friction stir spot welds fabricated by scroll grooved tool without probe, Sci. Technol. Weld. Join. 17 (2012) 348–356.
[25] S. Bozzi, A.L. Etter, T. Baudin, V. Klosek, J.G. Kerbiguet, B. Criqui, Influence of FSSW parameters on fracture mechanisms of 5182 aluminium welds, J. Mater. Process. Technol. 210 (2010) 1429–1435.
[26] R.Z. X u, D.R. Ni, Q. Yang, C.Z. Liu, Z.Y. Ma, Influence of Zn interlayer addition on microstructure and mechanical properties of friction stir welded AZ31 Mg alloy, J. Mater. Sci. 50 (2015) 4160–4173.
[27] C. Schneider, T. Weinberger, J. Inoue, T. Koseki, N. Enzinger, Characterisation of interface of steel/magnesium FSW, Sci. Technol. Weld. Join. 16 (2011) 100–106.
[28] Y.C. Chen, K. Nakata, Effect of tool geometry on microstructure and mechanical properties of frictionstir lap welded magnesium alloy and steel, Mater. Des. 30 (2009) 3913–3919.
[29] Y.C. Chen, K. Nakata, Friction stir lap welding of magnesium alloy and zinc-coated steel, Mater. Trans. 50 (2009) 2598–2603.
[30] T. Liyanage, J. Kilbourne, A.P. Gerlich, T.H. North, Joint formation in dissimilar Al alloy/steel and Mg alloy-steel friction stir spot welds, Sci. Technol. Weld. Join. 14 (2009) 500–508.
[31] R.Z. Xu, D.R. Ni, Q. Yang, C.Z. Liu, Z.Y. Ma, Influencing mechanism of Zn interlayer addition on hook defects of friction stir spot welded Mg–Al–Zn alloy joints, Mater. Des. 69 (2015) 163–169.
[32] A.R. Marder, The metallurgy of zinc-coated steel, Prog. Mater. Sci. 45 (2000) 191–271.